Chemical Engineering Journal 260 (2015) 791–800

Contents lists available at ScienceDirect

Chemical Engineering Journal

journal homepage: www.elsevier.com/locate/cej

Effect of high orthophosphate concentration on mesophilic anaerobic sludge digestion and its modeling

Ruyi Wang [a,b], Yongmei Li [a,*], Wenhan Wang [a], Yinguang Chen [a], Peter A. Vanrolleghem [b,*]

[a] State Key Laboratory of Pollution Control and Resource Reuse, Tongji University, Shanghai 200092, China
[b] modelEAU, Département de génie civil et de génie des eaux, Université Laval, 1065 av. de la Médecine, Québec, QC G1V 0A6, Canada

HIGHLIGHTS

- Orthophosphate affects methanogenesis, acetogenesis and acidogenesis.
- Haldane kinetics of orthophosphate inhibition is proposed for inclusion in ADM1.
- Parameters of the new model are estimated from an extensive data set.
- The new model fits the measured data well and is validated on independent data.

GRAPHICAL ABSTRACT

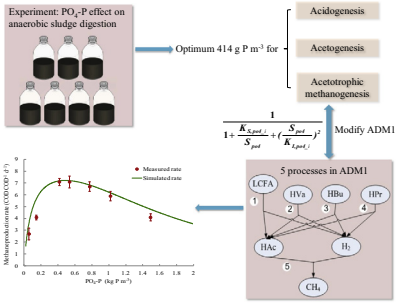

ARTICLE INFO

Article history:
Received 17 February 2014
Received in revised form 11 September 2014
Accepted 15 September 2014
Available online 22 September 2014

Keywords:
Acetate inhibition
ADM1
Enhanced biological phosphorus removal
Haldane kinetics
Mesophilic anaerobic digestion
Orthophosphate inhibition

ABSTRACT

To gain insight regarding the orthophosphate influence on fatty acid dynamics and methane production during mesophilic anaerobic sludge digestion, batch experiments were conducted. The results showed that an orthophosphate concentration of 414 g P m^{-3} accelerated acetotrophic methanogenesis, acetogenesis and acidogenesis. Lower or higher concentrations slowed these processes down. Three modifications of the Anaerobic Digestion Model No. 1 (ADM1) were compared by simultaneously fitting them to a multi-experiment (7 batches), multi-variable (6 measured variables) data set. A modified ADM1 model including Haldane kinetics of orthophosphate inhibition gave the best description of the measured data while the model using non-competitive acetate inhibition showed the poorest results. It is notable that the multi-experiment, multi-variable data set could be fitted with a single parameter set. The model with Haldane kinetics of orthophosphate inhibition together with the proposed parameters can be considered as a first attempt to describe the observed orthophosphate inhibition of anaerobic digestion.

1. Introduction

Phosphorus removal from wastewater is important for preventing natural waters from eutrophication. Chemical or biological processes are usually used for phosphorus removal from wastewater. Many wastewater treatment plants are designed using the enhanced biological phosphorus removal (EBPR) process, which is based on biological uptake and transfer of phosphorus from the liquid phase to the sludge phase in excess of the amount that is removed by traditional aerobic activated sludge systems [1]. The amount of phosphorus incorporated in the EBPR sludge mass is increased from the normal value of 0.02 mg P mg VSS^{-1} to 0.06–0.15 mg P mg VSS^{-1} (0.05–0.10 mg P mg TSS^{-1}) [2]. The phosphorus-rich sludge subsequently needs to be treated and disposed of.

* Corresponding authors. Tel.: +86 021 65982692; fax: +86 21 65986313 (Y. Li). Tel.: +1 418 656 5085; fax: +1 418 656 2928 (P.A. Vanrolleghem).
E-mail addresses: liyongmei@tongji.edu.cn (Y. Li), Peter.Vanrolleghem@gci.ulaval.ca (P.A. Vanrolleghem).

http://dx.doi.org/10.1016/j.cej.2014.09.050
1385-8947/

The world-wide application of anaerobic digestion is rapidly growing, since anaerobic digestion has the ability to reduce the overall amount of biosolids to be disposed of by more than 40% while producing an energy-rich biogas (around 65% methane) [2,3]. It was revealed that more than 80% of the total biologically-bound phosphorus that had been removed previously during EBPR treatment was released during anaerobic digestion and up to 1500 g P m^{-3} soluble phosphorus can be observed in anaerobic digesters [4,5].

Bacteria, especially methanogenic bacteria, in anaerobic digestion are sensitive to their living conditions. Nutrients in the medium are vital to bacterial growth. One of the most important nutrients is phosphorus. It is one of the major constituents of living organisms and plays an important role in their metabolism. Therefore, it is significant to investigate whether and how bacteria are affected by such high phosphate concentrations in anaerobic digestion treating phosphorus-rich sludge. Surprisingly, few studies have been conducted on the phosphate effect on the reactions mediated by bacteria during anaerobic digestion. Rudolfs and Stahl [6] pointed out that the amount of phosphorus added exerted a retarding effect on gas production up to a certain concentration and increasing quantities of phosphorus caused greater inhibition of biological activities. A decreased rate of gas production with addition of phosphate buffer (2170, 4650, and 7130 g P m^{-3}) compared with that without additional phosphate (186 g P m^{-3}) was found by Van Den Berg et al. [7]. A study on the effect of phosphate supplementation on methane production from rice reported that a level of phosphate addition (465 g P m^{-3}) could accelerate the biogasification process [8] and addition of more than 620 g P m^{-3} of phosphate in the media inhibited methanogenesis [9]. However, the effect of phosphate on different processes of anaerobic sludge digestion including acidogenesis, acetogenesis and methanogenesis as well as the relationship of phosphate concentration and anaerobic digestion processes are still not well explored.

Anaerobic digestion models have been proposed since the end of the 1960s [10,11]. The Anaerobic Digestion Model No. 1 (ADM1) was developed as a unified base for modeling of anaerobic digestion [12]. Although some adjustments and extensions based on ADM1 have been made since then [13,14], the phosphate effect is hardly considered in anaerobic digestion models. Therefore, establishing a mathematical relationship between phosphate concentration and anaerobic digestion processes is beneficial to better understanding and optimizing the anaerobic digestion process for sludge treatment.

The objective of this study was to gain insight regarding the orthophosphate influence on biological processes during mesophilic anaerobic sludge digestion. Batch experiments were conducted to investigate the effect of orthophosphate concentrations on acidogenesis, acetogenesis and methanogenesis during the anaerobic digestion process. The obtained experimental results were used for the establishment of kinetics expressions, in the framework of the ADM1.

2. Materials and methods

2.1. Experimental set-up

Two sets of batch experiments were carried out. Experimental set A was conducted in identical serum bottles with a volume of 600 mL in a temperature controlled shaker (35 ± 1 °C). Each serum bottle contained 450 mL of digested sludge inoculum and 50 mL of synthetic sludge (starch 7 kg m^{-3}, toilet paper 10 kg m^{-3}, coffee creamer 11 kg m^{-3}, high fibre bran 12 kg m^{-3}, peptone 1 kg m^{-3}, yeast extract 3 kg m^{-3}, $NaHCO_3$ 3 kg m^{-3}) [15]. The digested sludge inoculum was obtained from a laboratory-scale anaerobic digester fed with waste activated sludge. The anaerobic sludge was washed and diluted with distilled water prior to its use so as to decrease the orthophosphate level. The characteristics of the mixed sludge are shown in Table 1. Soluble phosphorus (as Na_2HPO_4 and NaH_2PO_4) was added to make soluble PO_4-P concentrations of 144, 414, 535, 773, 1017, and 1489 g P m^{-3} (average values of the orthophosphate concentrations measured over time throughout the experiment). The bottle without addition of soluble phosphorus, in which the concentration of soluble PO_4-P was 57 g P m^{-3}, was labeled as Control-57. Samples were taken for analysis after gas was sampled, and then the pH value in each bottle was controlled at 7.0 ± 0.1 by adding KOH or HCl. Anaerobic conditions were achieved by purging with nitrogen gas for 20 s. The batch experiments were performed in triplicate, and their averages are reported.

For model validation, experimental set B with the same digested sludge inoculum and synthetic sludge was carried out. Soluble phosphorus (as Na_2HPO_4 and NaH_2PO_4) was added to make concentrations of soluble PO_4-P of 545 g P m^{-3}. The bottle without addition of soluble phosphorus, in which the concentration of soluble PO_4-P was 125 g P m^{-3}, was labeled as Control-125. The bottles were maintained in a temperature controlled shaker (35 ± 1 °C). In order to test the proposed model under non-pH-controlled conditions, pH values in both bottles were not controlled.

2.2. Analysis

Samples from the bottles were immediately filtered through a Whatmann GF/C glass microfiber filter. The filtrate was analyzed for volatile fatty acids (VFAs), SCOD, STOC, STN, PO_4-P, NH_4-N, and the filter residue was assayed for TSS and VSS. STOC and STN were determined by a TOC analyzer (TOC-V CPH; Shimadzu). Methane and VFAs were measured by gas chromatography [16]. The analyses of PO_4-P, NH_4-N, COD, TSS, and VSS were conducted according to standard methods [17].

2.3. Modeling approach

Models of the different processes were modified according to the experimental results with ADM1 as basic model, applying the same structure, nomenclature, and units [12]. Three ADM1 modifications were compared by simultaneously fitting them to measured data (Table 2). ADM1 was extended by introducing generalized Haldane equations of orthophosphate inhibition into the uptake process kinetics of acetate, propionate, butyrate, valerate, and long-chain fatty acids (LCFA) and was named M1. ADM1 modified by introducing non-competitive inhibition of acetate into the uptake process kinetics of LCFA, butyrate (valerate), and propionate was named M2, and the model with combined inhibition of orthophosphate and acetate into the same processes was named

Table 1
Characterization of the mixture of digested sludge inoculum and synthetic sludge.

Parameter	Description	Value	Unit
TSS	Total suspended solids	9270 ± 502	g m^{-3}
VSS	Volatile suspended solids	7090 ± 388	g m^{-3}
TCOD	Total chemical oxygen demand	9625 ± 629	g COD m^{-3}
SCOD	Soluble chemical oxygen demand	1350 ± 83	g COD m^{-3}
STOC	Soluble total organic carbon	615 ± 38	g C m^{-3}
STN	Soluble total nitrogen	53 ± 5	g N m^{-3}
VFAs	Volatile fatty acids	75 ± 5	g COD m^{-3}
S_{ac}	Acetate	44 ± 3	g COD m^{-3}
S_{pro}	Propionate	20 ± 1	g COD m^{-3}
S_{bu}	Butyrate	11 ± 1	g COD m^{-3}
S_{va}	Valerate	0	g COD m^{-3}
S_{NH_4}	Ammonium	18 ± 1	g N m^{-3}

Table 2
Process rate modifications in the three proposed ADM1 extensions.

Model approach	Process	Rate equation	Eq. No.
M1, M2, M3	S_{ac} uptake	$\rho_{11} = k_{m,ac}\frac{S_{ac}}{K_s+S_{ac}}\frac{1}{1+\frac{K_{S,po4\_ac}}{S_{po4}}+\left(\frac{S_{po4}}{K_{I,po4\_ac}}\right)^2}X_{ac}I_{pH}I_{IN,lim}I_{NH_3,Xac}$	(7)
M1	S_{pro} uptake	$\rho_{10} = k_{m,pro}\frac{S_{pro}}{K_s+S_{pro}}\frac{1}{1+\frac{K_{S,po4\_pro}}{S_{po4}}+\left(\frac{S_{po4}}{K_{I,po4\_pro}}\right)^2}X_{pro}I_{pH}I_{IN,lim}I_{h2}$	(8)
	S_{bu} and S_{va} uptake	$\rho_{9(or\ 8)} = k_{m,c4}\frac{S_{bu}(orS_{va})}{K_s+S_{bu}(orS_{va})}\frac{1}{1+\frac{S_{va}}{S_{bu}}\left(or\frac{S_{bu}}{S_{va}}\right)}\frac{1}{1+\frac{K_{S,po4\_c4}}{S_{po4}}+\left(\frac{S_{po4}}{K_{I,po4\_c4}}\right)}X_{c4}I_{PH}I_{IN,lim}I_{h2}$	(9)
	S_{fa} uptake	$\rho_7 = k_{m,fa}\frac{S_{fa}}{K_s+S_{fa}}\frac{1}{1+\frac{K_{S,po4\_fa}}{S_{po4}}+\left(\frac{S_{po4}}{K_{I,po4\_fa}}\right)^2}X_{fa}I_{pH}I_{IN,lim}I_{h2}$	(10)
M2	S_{pro} uptake	$\rho_{10} = k_{m,pro}\frac{S_{pro}}{K_s+S_{pro}}\frac{K_{I,ac\_pro}}{K_{I,ac\_pro}+S_{ac}}X_{pro}I_{pH}I_{IN,lim}I_{h2}$	(11)
	S_{bu} and S_{va} uptake	$\rho_{9(or\ 8)} = k_{m,c4}\frac{S_{bu}(orS_{va})}{K_s+S_{bu}(orS_{va})}\frac{1}{1+\frac{S_{va}}{S_{bu}}\left(or\frac{S_{bu}}{S_{va}}\right)}\frac{K_{I,ac\_c4}}{K_{I,ac\_c4}+S_{ac}}X_{c4}I_{pH}I_{IN,lim}I_{h2}$	(12)
	S_{fa} uptake	$\rho_7 = k_{m,fa}\frac{S_{fa}}{K_s+S_{fa}}\frac{K_{I,ac\_fa}}{K_{I,ac\_fa}+S_{ac}}X_{fa}I_{pH}I_{IN,lim}I_{h2}$	(13)
M3	S_{pro} uptake	$\rho_{10} = k_{m,pro}\frac{S_{pro}}{K_s+S_{pro}}\frac{1}{1+\frac{K_{S,po4\_pro}}{S_{po4}}+\left(\frac{S_{po4}}{K_{I,po4\_pro}}\right)^2}\frac{K_{I,ac\_pro}}{K_{I,ac\_pro}+S_{ac}}X_{pro}I_{pH}I_{IN,lim}I_{h2}$	(14)
	S_{bu} and S_{va} uptake	$\rho_{9(or\ 8)} = k_{m,c4}\frac{S_{bu}(or\ S_{va})}{K_s+S_{bu}(or\ S_{va})}\frac{1}{1+\frac{S_{va}}{S_{bu}}\left(or\frac{S_{bu}}{S_{va}}\right)}\frac{1}{1+\frac{K_{S,po4\_c4}}{S_{po4}}+\left(\frac{S_{po4}}{K_{I,po4\_c4}}\right)^2}\frac{K_{I,ac\_c4}}{K_{I,ac\_c4}+S_{ac}}X_{c4}I_{pH}I_{IN,lim}I_{h2}$	(15)
	S_{fa} uptake	$\rho_7 = k_{m,fa}\frac{S_{fa}}{K_s+S_{fa}}\frac{1}{1+\frac{K_{S,po4\_fa}}{S_{po4}}+\left(\frac{S_{po4}}{K_{I,po4\_fa}}\right)^2}\frac{K_{I,ac\_fa}}{K_{I,ac\_fa}+S_{ac}}X_{fa}I_{pH}I_{IN,lim}I_{h2}$	(16)

The value of the constant determining the inhibition order in the generalized Haldane equation ($n = 2$) was estimated according to experimental data. Nomenclature and units were maintained from ADM1 [12].

M3. The acetate uptake process kinetics in M2 and M3 was modified by introducing the Haldane equation of orthophosphate inhibition as well. The rate coefficients of these 5 processes are the same as those of the original ADM1 (Table S1). The default values for the kinetic parameters and stoichiometric coefficients suggested by Batstone et al. [12] were adopted except for a number of kinetic parameters, the values of which were determined from the experimental data (Table 3). Initial particulate COD was mainly present in the form of composites (X_c), carbohydrates (X_{ch}), proteins (X_{pr}), lipids (X_{li}), particulate inerts (X_I), and some biomass. Most initial substrate concentrations were directly obtained from the experimental measurements. The initial values that could not be measured directly were calculated from the available values based on the COD and nitrogen balance, and were determined by fitting to the curves of measured variables. Especially the initial concentration of each biomass species was mainly determined by fitting to the curve of its corresponding substrate. Except for orthophosphate concentration, the same initial concentrations were applied to every batch test simulation. Modeling and simulation were carried out using the WEST software (Mikebydhi.com).

For pH simulation, only the second orthophosphate dissociation reaction (1) was considered since the orthophosphate species in anaerobic digestion almost entirely comprises of $H_2PO_4^-$ and HPO_4^{2-} in the pH range of 4–10 [18]. To account for pH inhibition (I_{pH}), a Hill inhibition function based on the hydrogen ion concentration (S_H^+), shown as Eq. (2), was applied in ADM1 [19]. The $pH_{LL} = 5.6$ (inhibition is complete at pH 5.6) and $pH_{UL} = 7$ (inhibition starts below pH 7) was used for acetate uptake as suggested by Siegrist et al. [19]. The default values for the pH inhibition parameters of the other processes as suggested by Batstone et al. [12] were adopted.

$$H_2PO_4^- \leftrightarrow HPO_4^{2-} + H^+ \quad (1)$$

$$I_{pH} = \frac{K_{pH}^n}{S_H^{+n} + K_{pH}^n}, \text{ with } K_{pH} = 10^{-\frac{pH_{LL}+pH_{UL}}{2}} \quad (2)$$

2.4. Calibration approach

To fit a model to the data, the objective function was minimized according to the weighted least squared objective function Eq. (3) for fitting a single model to a multi-experiment, multi-variable data set [20,21].

Table 3
Values of estimated parameters for the three ADM1 model extentions.

No.	Parameter	M1	M2	M3	ADM1	Unit	Description
1	$k_{m,ac}$	9.7	9.7	9.7	8	kg COD kg COD^{-1} d^{-1}	Monod maximum specific acetate uptake rate
2	$K_{S,po4\_ac}$	0.09	0.09	0.09	–	kg P m^{-3}	Orthophosphate saturation constant for acetate uptake
3	$K_{I,po4\_ac}$	1.6	1.6	1.6	–	kg P m^{-3}	Orthophosphate inhibition constant for acetate uptake
4	$k_{m,c4}$	13.5	11.5	20	20	kg COD kg COD^{-1} d^{-1}	Monod maximum specific valerate and butyrate uptake rate
5	$K_{S,po4\_c4}$	0.08	–	0.08	–	kg P m^{-3}	Orthophosphate saturation constant for valerate and butyrate uptake
6	$K_{I,po4\_c4}$	1.7	–	1.7	–	kg P m^{-3}	Orthophosphate inhibition constant for valerate and butyrate uptake
7	$k_{m,pro}$	7.2	6.7	8.5	13	kg COD kg COD^{-1} d^{-1}	Monod maximum specific propionate uptake rate
8	$K_{S,po4\_pro}$	0.04	–	0.04	–	kg P m^{-3}	Orthophosphate saturation constant for propionate uptake
9	$K_{I,po4\_pro}$	1.8	–	1.8	–	kg P m^{-3}	Orthophosphate inhibition constant for propionate uptake
10	$k_{m,fa}$	6.7	5	8.3	6	kg COD kg COD^{-1} d^{-1}	Monod maximum specific LCFA uptake rate
11	$K_{S,po4\_fa}$	0.11	–	0.11	–	kg P m^{-3}	Orthophosphate saturation constant for LCFA uptake
12	$K_{I,po4\_fa}$	1.8	–	1.8	–	kg P m^{-3}	Orthophosphate inhibition constant for LCFA uptake
13	K_{I,ac_c4}	–	1.5	1.5	–	kg COD m^{-3}	Acetate inhibition constant for valerate and butyrate uptake
14	K_{I,ac_pro}	–	1.3	1.3	–	kg COD m^{-3}	Acetate inhibition constant for propionate uptake
15	K_{I,ac_fa}	–	1	1	–	kg COD m^{-3}	Acetate inhibition constant for LCFA uptake

$$J = \sum_{k=1}^{N_{bot}} \sum_{j=1}^{N_{vark}} w_{jk} \sum_{i=1}^{N_{datajk}} (y_{ijk} - \hat{y}_{ijk})^2 \quad (3)$$

$$w_{jk} = \left[N_{datajk} (\max(y_{ijk}) - \min(y_{ijk}))^2 \right]^{-1} \quad (4)$$

where y_{ijk} represents the measured value of variable j, in bottle k, at time i, and $\hat{y}_{ijk}$ is the corresponding simulated value. Variable j from bottle k has N_{datajk} measured values at successive different times i. N_{vark} and N_{bot} are the number of variables and bottles, respectively. w_{jk} is the weight factor (Eq. (4)). $\max(y_{ijk})$ and $\min(y_{ijk})$ are the maximum and minimum measured value among all values of variable j in bottle k, respectively. In total 7 parallel experiments, in which each time 6 variables (methane, valerate, butyrate, propionate, acetate, and SCOD after deduction of VFAs) were measured, were used to fit the models.

The selection of the best model was based on the number of measured data as well as the goodness-of-fit and the number of parameters of the models. This was done with Akaike's Information Criterion (AIC), shown as Eq. (5) [20].

$$\mathrm{AIC} = N \log\left(\frac{J}{N}\right) + 2p \quad (5)$$

where p represents the number of fitted parameters in the parameter estimation (shown in Table 3), N is the total number of measured data, and J is given by Eq. (3). Lower values of AIC correspond to better model performance.

The goodness-of-fit between experimental (y_{ijk}) and simulated values ($\hat{y}_{ijk}$) for a variable j using the optimized parameters was also quantified by calculating Theil's inequality coefficient (TIC), shown as Eq. (6) [22].

$$\mathrm{TIC}_{jk} = \frac{\sqrt{\frac{1}{N_{datajk}} \sum_{i=1}^{N_{datajk}} (y_{ijk} - \hat{y}_{ijk})^2}}{\sqrt{\frac{1}{N_{datajk}} \sum_{i=1}^{N_{datajk}} (y_{ijk})^2} + \sqrt{\frac{1}{N_{datajk}} \sum_{i=1}^{N_{datajk}} (\hat{y}_{ijk})^2}} \quad (6)$$

TIC allows judging whether there is a considerable difference between simulated and measured results. A value of the TIC less than 0.3 indicates a good agreement with measured data.

3. Results

3.1. Effect of orthophosphate

After 61-d anaerobic digestion, the methane yields of batch experimental set A varied between 0.28 and 0.35 m^3 CH_4 kg VSS^{-1}. The concentrations of PO_4-P remained relatively stable during the experiment (Fig. S1), while the concentrations of NH_4-N increased gradually to 180–197 g N m^{-3}.

The cumulative methane productions with additional orthophosphate were all higher than Control-57, which is reflected in the cumulative methane productions those were normalized against Control-57 and those were all higher than 1 (Fig. 1). It is obvious that during the first 30 days the methane production went faster with an increase of orthophosphate concentration from 57 to 414 g P m^{-3}, and slowed down again with further increase of orthophosphate concentration. The highest methane production occurred for P-414, followed by P-535 and P-773 during the first 30 days. The methane production for P-414 was 5.4 times greater than that produced by Control-57 during the first 13 days. The normalized cumulative methane production for P-414 decreased between day 10 and 30 because the acetate concentration for P-414 became very low and became a limiting factor while the acetate concentration for Control-57 still remained high (Fig. 2). Similarly, the normalized cumulative methane production for the other 5 bottles also decreased but occurred at later dates. Such

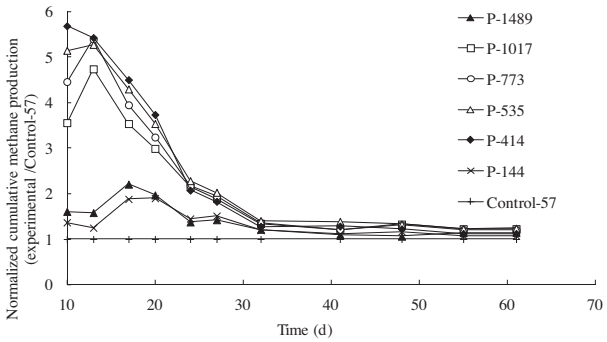

Fig. 1. Normalized cumulative methane production from batch digesters containing different concentrations of PO_4-P. Normalization with respect to Control-57.

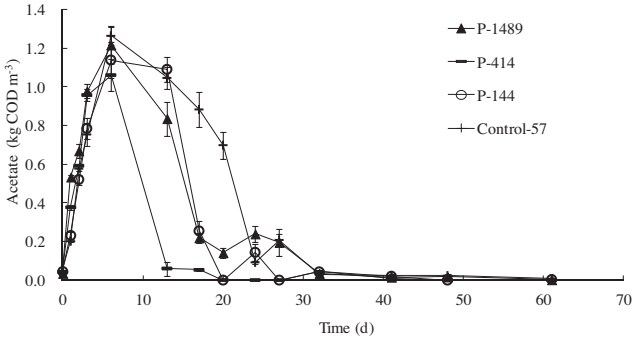

Fig. 2. Measured acetate concentration profiles at different orthophosphate concentrations. Error bars represent standard deviations (n = 3).

results indicate that the orthophosphate concentration of 414 g P m^{-3} accelerated methane production; lower or higher concentrations slowed the progress down.

Acetate accumulation started right away because of the hydrolysis of organic substances (Fig. 2). After 6-d operation, the acetate concentration for P-414 decreased sharply at the highest rate, while it decreased at the slowest rate for Control-57. The acetate concentration profile for P-1489 was similar to that for P-144. The acetate decreased faster with an increase of orthophosphate concentration from 57 to 414 g P m^{-3}, and slowed down again with further increase of orthophosphate concentration. Such trend is the same with that of methane production (Fig. 1). On the contrary, under all conditions hydrogen was undetectable except that a very little was observed on the first day. This indicates that hydrogen produced from acetogenesis and acidogenesis processes was instantly consumed. Thus, the hydrogen uptake process was limited by the availability of hydrogen no matter what the orthophosphate concentration was. Therefore, the results reveal that in this study the orthophosphate concentration affected methanogenesis mainly by influencing the acetate uptake process.

As shown in Figs. 3 and 4, the variations of cumulative methane production correlated well with those of organic substances. For example, P-1489 exhibited a high methane production during the first 20 days because of the availability of acetate. As acetate was depleted, butyrate and valerate, followed by the SCOD (after deduction of total VFAs, i.e. LCFA, sugars, amino acids, and soluble inerts) contributed to the further increase in methane production for P-1489 during 20–40 days. The final stage of methane production for P-1489 arose from propionate use. It is worth noting that the depletion of the soluble organic substances (propionate, butyrate, valerate, and the SCOD after deduction of total VFAs), like that of acetate, went faster with an increase of orthophosphate concen-

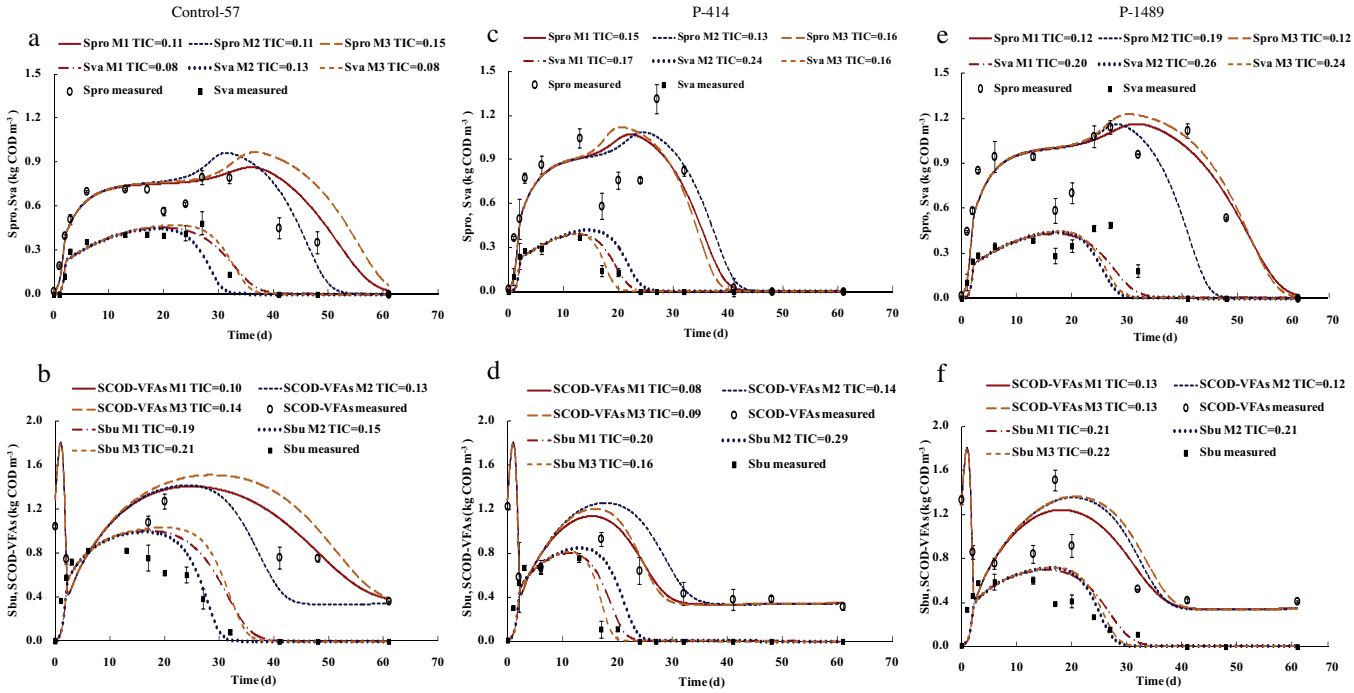

Fig. 3. Experimental data (markers) and different model results (lines, M1: Haldane kinetics of orthophosphate inhibition for process rates ρ_{7-11}; M2: non-competitive inhibition of acetate for process rates ρ_{7-10} and Haldane kinetics of orthophosphate inhibition for process rate ρ_{11}; M3: both Haldane kinetics of orthophosphate inhibition and non-competitive inhibition of acetate for process rates ρ_{7-10} and Haldane kinetics of orthophosphate inhibition for process rate ρ_{11}) for Control-57 (a and b), P-414 (c and d), and P-1489 (e and f) in terms of propionate (S_{pro}), valerate (S_{va}), butyrate (S_{bu}), and SCOD after deduction of total VFAs (SCOD − VFAs). TIC coefficients for model fitting are indicated in every plot. Error bars represent standard deviations ($n = 3$).

tration from 57 to 414 g P m^{-3}, and slowed down again with further increase of orthophosphate concentration (Figs. 2 and 3). These results thus indicate that an adequate level of orthophosphate concentration (414 g P m^{-3}) accelerates acidogenesis, acetogenesis, and acetotrophic methanogenesis, while a further increase of the orthophosphate concentration slows these processes down.

3.2. Mathematical modeling

3.2.1. Modeling the effect of orthophosphate

When ADM1 was applied as such, the simulation results at different orthophosphate would be the same since no orthophosphate effect is included in ADM1. Therefore, according to the experimental results, ADM1 was extended to describe the observations by introducing generalized Haldane equations of orthophosphate inhibition into acetate, propionate, butyrate, valerate, and LCFA uptake processes (Table 2). Since the uptake rates of sugars and amino acids were much higher than that of LCFA, the simulated sugars and amino acids were totally degraded within the first 2 days despite hydrolysis of carbohydrates and proteins, while LCFA accumulated for a period of time. This indicates that the accumulation and depletion of LCFA was the main contributor to the variation of SCOD after deduction of total VFAs over time, especially after the first 2 days. Therefore, it was assumed that orthophosphate mainly affected the LCFA uptake process during the acidogenesis stage. According to the measured results, the effect of orthophosphate on the hydrogen uptake process was not considered in the extended ADM1, but the methane produced from this process was simulated. Initially a constant pH value 7 was applied to investigate the effect of varying orthophosphate concentrations. Table 3 provides the parameter values estimated according to the above batch experimental data.

Fig. 5 shows the effect of the orthophosphate concentration on the maximum methane production rate. It is obvious that the predicted methane production rates corresponded well with the experimental rates. The data in Fig. 5 indicate that the methane production rate substantially increases when the orthophosphate concentration increases from 0.057 to 0.414 kg P m^{-3} while it decreases with a further increase of orthophosphate concentration (optimum methane production rate was achieved at orthophosphate concentrations between 0.3 and 0.6 kg P m^{-3}). M1 simulations closely followed the dynamic evolutions of the main variables (Figs. 3 and 4). The TIC values of the simulated results (M1) range from 0.02 to 0.24 (all the TIC values are shown in Table S2), below the limit value of 0.3 [22]. Especially the TIC of each cumulative methane production result is less than 0.06.

3.2.2. Model comparison

It was reported that degradation of fatty acids may be inhibited by high concentrations of acetate, and non-competitive inhibition of acetate was proposed [19,23–25]. Therefore, ADM1 was modified by introducing non-competitive inhibition of acetate (M2) and combined inhibition of orthophosphate and acetate (M3) into LCFA, butyrate (valerate), and propionate uptake processes. The three models (M1, M2, and M3 shown in Table 2) were compared by fitting them to the experimental data in order to find out which one describes the experimental data best.

M1 simulations of the considered variables were superior to simulations of the other two models and were in good agreement with the observed variables (Figs. 3 and 4). Although the TIC values of M2 were also all lower than 0.3 and the M2 simulated profiles of variables were acceptable in some cases, it was hard to find a unique set of parameters capable of fitting all experimental data as well as M1 did. The differences between measurements and simulations of M2 were more noticeable at low (57 g P m^{-3}) and high (1489 g P m^{-3}) orthophosphate concentrations (Figs. 3 and 4). The profiles of variables simulated by M3 were similar to those by M1, but the TIC values of M3 were slightly higher in most cases (Figs. 3, 4, and Table S2).

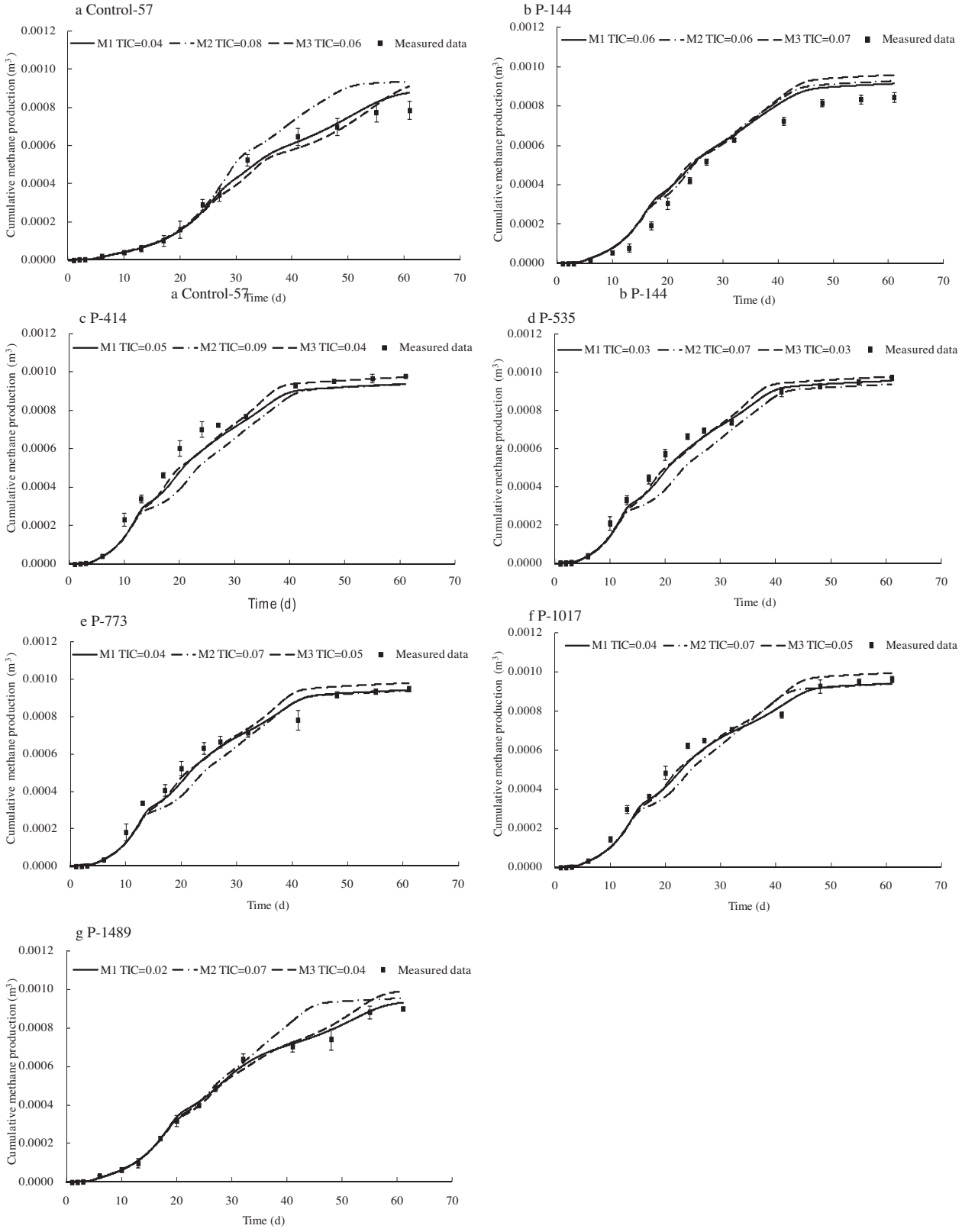

Fig. 4. Experimental data (markers) and different model results (lines, M1: Haldane kinetics of orthophosphate inhibition for process rates ρ_{7-11}; M2: non-competitive inhibition of acetate for process rates ρ_{7-10} and Haldane kinetics of orthophosphate inhibition for process rate ρ_{11}; M3: both Haldane kinetics of orthophosphate inhibition and non-competitive inhibition of acetate for process rates ρ_{7-10} and Haldane kinetics of orthophosphate inhibition for process rate ρ_{11}) in terms of cumulative methane production. TIC coefficients for model fitting are indicated in every plot. Error bars represent standard deviations ($n = 3$).

The model of orthophosphate inhibition (M1, AIC = −1464) gave the best description of the measured data while the acetate inhibition model (M2, AIC = −1368) gave the poorest. Although M1 has a larger number of parameters than M2, the AIC value of M1 was the lowest due to the lowest J value ($J = 1.023$), which was 35% less than that of M2 ($J = 1.565$). The most significant point is that the

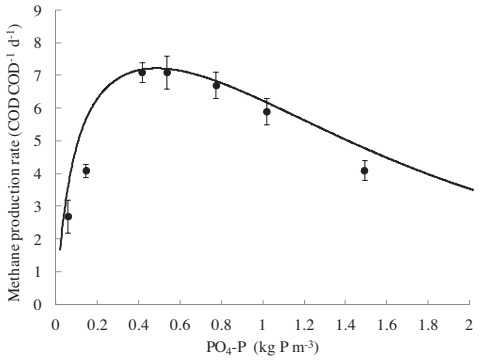

Fig. 5. Methane production rates from batch digesters containing different concentrations of PO_4-P calculated from experimental data (markers) and predicted by the adjusted acetate uptake rate considering Haldane kinetics of orthophosphate inhibition (line). Error bars represent standard deviations (n = 3).

AIC value of M2 was the highest despite the fact that M2 employed the fewest parameters (9). The AIC value (−1406) of M3 considering both orthophosphate and acetate inhibition was also higher than that of M1, i.e. there is no need to add acetate inhibition to get a better description.

3.2.3. Modeling the effect of pH

As shown in Figs. 6 and S2, within the first few days pH values dropped in between the manual pH corrections due to acidification. They got stable after 10 days. Also, the pH values within the first few days became more stable and close to neutral with the increase of orthophosphate concentration and the corresponding increase in buffer capacity. To investigate pH inhibition especially for the experiments at relatively low orthophosphate concentrations, pH was applied as an additional variable to M1 (Eq. (2)). The TIC values of the simulated pH values were less than 0.02, indicating that good simulation of pH variations was obtained (Fig. 6). Since the buffer capacity at Control-57 was low compared with those in the other bottles, relatively large pH drops occurred during the first 10 days. However, the TIC value of cumulative methane production considering pH variation was only slightly higher than that without considering pH inhibition for Control-57 (Fig. 7). For P-144, the simulated results got slightly better by considering pH inhibition. The TIC values of cumulative methane production with and without considering true pH variation were the same for P-414, indicating that the pH effect was negligible. In summary, these simulation results show that the pH effect on methane production was not significant in the tested orthophosphate concentration range (57–1489 g P m^{-3}), and it became negligible as the orthophosphate concentration increased above 414 g P m^{-3}.

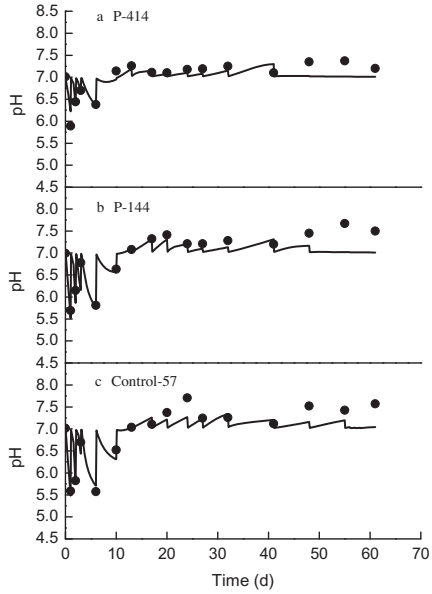

Fig. 6. Experimental (markers) and simulated pH variations (lines) in the anaerobic digester for orthophosphate concentrations of 414 g P m^{-3} (a), 144 g P m^{-3} (b), and 57 g P m^{-3} (c), $TIC_{P\text{-}414}$ = 0.01, $TIC_{P\text{-}144}$ = 0.02, $TIC_{Control\text{-}57}$ = 0.02. The relative standard deviations (n = 3) were less than 2%.

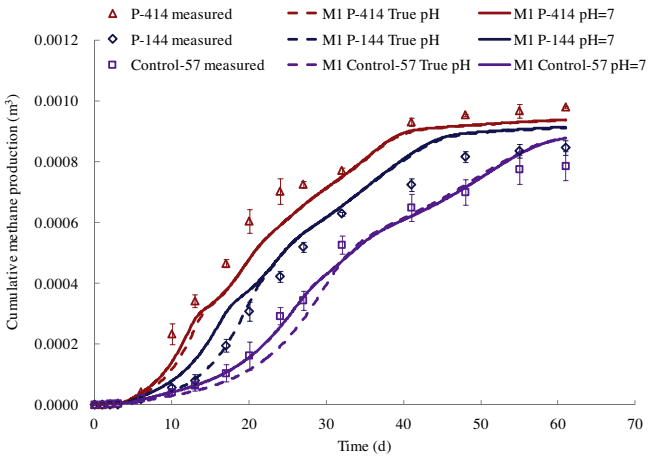

Fig. 7. Experimental and simulated cumulative methane productions with and without considering pH inhibition for orthophosphate concentrations of 414 g P m^{-3} ($TIC_{true\ pH}$ = 0.05 $TIC_{pH=7}$ = 0.05), 144 g P m^{-3} ($TIC_{true\ pH}$ = 0.04 $TIC_{pH=7}$ = 0.06), and 57 g P m^{-3} ($TIC_{true\ pH}$ = 0.06 $TIC_{pH=7}$ = 0.04). Error bars represent standard deviations (n = 3).

3.3. Validation of ADM1 model modified by orthophosphate inhibition

The calibrated orthophosphate inhibition model M1, which is the most adequate one among the three tested models, was validated using the results of batch experimental set B, in which pH was not controlled to create different process conditions (Fig. 8). The simulated data for pH and cumulative methane production (obtained with the previously estimated parameter values) corresponded well with the experimental data (TIC $\leqslant$ 0.04). At an orthophosphate concentration of 545 g P m^{-3} and 125 g P m^{-3}, although started from the same initial pH values (7.8), the pH values in the two bottles differed from each other in terms of the extent of the pH drop and on the day exhibiting a sharp pH increase. The pH value for P-545 increased earlier and faster than that for Control-125, because the higher orthophosphate concentration created a higher buffer capacity on the one hand and on the other hand accelerated acetotrophic methanogenesis.

4. Discussion

4.1. Effect of orthophosphate concentration

The result obtained in the present study that the methane production rate had a maximum value in the orthophosphate concentration range of 300–600 g P m^{-3} confirms previous literature results [8,9]. Hardly any study was carried out before to investigate the effects of orthophosphate on acetogenesis and acidogenesis. Nevertheless, Lin and Lay [26] found that the hydrogen production ability of the anaerobic microbial ecosystem in sewage sludge was affected significantly by the phosphate concentration and had an optimal concentration at around 600 g Na_2HPO_4 m^{-3}. This finding

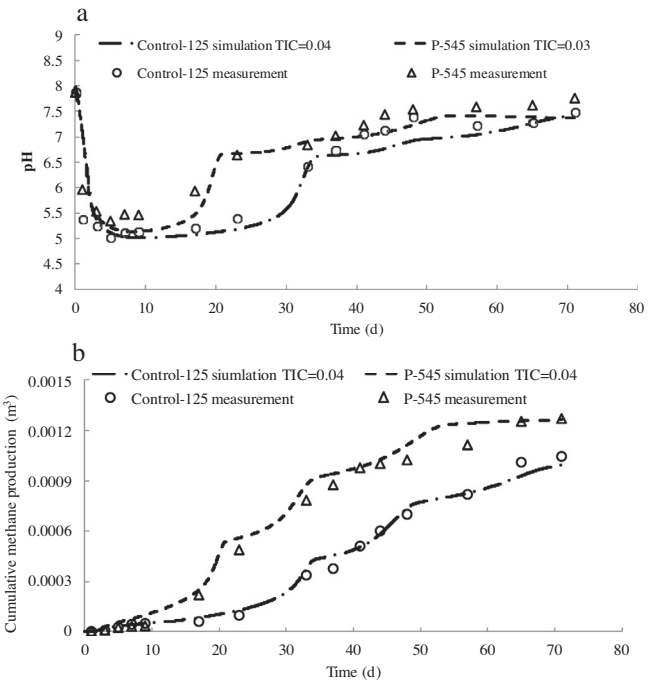

Fig. 8. Experimental and simulated M1-pH variations (a) and cumulative methane productions (b) for an orthophosphate concentration of 545 g P m^{-3} and 125 g P m^{-3}.

to some extent confirms the observations of this study that the acetogenesis and acidogenesis are affected by the orthophosphate concentration and have an optimum concentration around 414 g P m^{-3}, one of the concentrations tested.

So far no study was conducted to explain the phosphate effect on the anaerobic sludge digestion processes. In the field of antibiotic and secondary metabolites production by fermentation, it was reported that negative phosphate control of antibiotic biosynthesis in *Streptomyces lividans* and *Streptomyces coelicolor* is mediated by the two-component PhoR–PhoP system [27,28]. However, whether this mechanism can also explain the orthophosphate effect on anaerobic digestion needs further study, given the fact that it is still unknown whether methanogens are producers of secondary metabolites.

In order to investigate the effect of PO_4-P on anaerobic digestion, stable PO_4-P concentrations are needed and thus a mixture of a digested sludge inoculum and synthetic sludge was used. The synthetic sludge contributed to the observed increase of NH_4-N concentrations but no considerable change of PO_4-P concentrations was noticed during the experiment. Additionally, the concentrations of metal ions that may precipitate phosphate were low and stable during the operation (the average Mg^{2+} and Ca^{2+} concentrations at the first day and final day of all bottles were 21 ± 3 g m^{-3} and 27 ± 6 g m^{-3}, respectively). This indicates that precipitation was not important. The experimental results reveal that if the phosphorus precipitation in an anaerobic digester is considerable, making the orthophosphate concentration in the digester too low (less than 60 g P m^{-3}), sludge pre-treatment to enhance release of phosphorus could be considered in order to improve the performance of anaerobic digestion and to increase subsequent recovery of phosphorus as well. For the anaerobic digestion of EBPR waste activated sludge, cation availability (Mg^{2+}, Ca^{2+} and K^{+}), which can be co-released with phosphorus, will limit struvite and other mineral precipitation, and thus orthophosphate remains high [4,29]. Other options to limit phosphorus precipitation include alternative reactor configurations such as pre-acidification or digester pH adjustment through direct acid dosing [30]. On the contrary, if the orthophosphate concentration in the anaerobic digestion system is too high (more than 1500 g P m^{-3}), the orthophosphate concentration needs to be reduced before anaerobic sludge digestion. Fortunately, the orthophosphate concentrations in digesters range mostly between 100 and 500 g P m^{-3} depending on the type and amount of sludge treated [15].

4.2. Analysis of the kinetic parameters

The values of the Monod maximum specific uptake rate, $k_{m,i}$, were close to the default values and within the range suggested by Batstone et al. [12]. It should be noticed that the maximum value of the Haldane kinetics relation $\left(\frac{1}{1+\frac{K_{S,po4\_i}}{S_{po4}}+\left(\frac{S_{po4}}{K_{I,po4\_i}}\right)^2}\right)$ is less than 1. In this study, it ranged from 0.77 to 0.87 as calculated from the estimated parameter values given in Table 3. On the other hand, the maximum value of the non-competitive equation can be equal to 1 if the concentration of acetate is close to 0. This difference made the $k_{m,i}$ values of LCFA, butyrate (valerate), and propionate uptake processes in M2 to be slightly lower than the $k_{m,i}$ values in M1. Because of the dual effect of orthophosphate and acetate, the $k_{m,i}$ values of LCFA, butyrate (valerate), and propionate uptake processes in M3 were higher than those in M1 and M2.

A non-competitive acetate inhibition constant $K_{I,ac}$ = 1.5 - kg COD m^{-3} for degradation of LCFA and propionate was obtained by Siegrist et al. [19]. López and Borzacconi [24] used 0.96 kg m^{-3} as non-competitive acetate inhibition constant for propionate degradation and 0.72 kg m^{-3} as non-competitive acetate inhibition constant for butyrate degradation. The values of non-competitive acetate inhibition constants for LCFA, butyrate (valerate), and propionate uptake processes obtained in this study were similar to these literature data.

It can be calculated from the estimated values of $K_{S,spo4\_i}$ and $K_{I,spo4\_i}$ that the fatty acid uptake rates are only half of their maximum uptake rates when the orthophosphate concentrations are between 0.03 and 0.07 kg P m^{-3} or 2.0 and 2.2 kg P m^{-3}. The values of the orthophosphate saturation constant are surprising at first sight, because the values are much higher than the default value (0.01 g P m^{-3}) suggested for Activated Sludge Model No. 2 (ASM2) [31]. Since hardly any anaerobic digestion model described the orthophosphate effect so far, the value of an orthophosphate saturation constant for anaerobic digestion processes cannot be found in literatures. In general, the organic substrate half saturation constants of ADM1 (0.15–0.5 kg COD m^{-3}) are substantially higher than that in ASM2 (0.004 kg COD m^{-3}). The difference might result from differences in metabolic efficiency and from the dependence of the Monod half saturation constant on the biomass concentration, i.e. the constant would increase as the mass transfer limitations become more severe [32]. Another major reason for the high values of the orthophosphate half saturation constant in anaerobic digestion can be explained as follows.

The preferable source of phosphorus in bacteria is inorganic phosphate (Pi), which, depending on its concentration in the medium, is taken up by two different transport systems. When extracellular Pi is in excess, it is transported into the cell by the so-called low-affinity phosphate inorganic transport (Pit) system. But under phosphate-limiting conditions, Pi is transported by the high-affinity phosphate-specific transport (Pst) system, which is repressed by phosphate concentrations above 10^{-3} M (31 g P m^{-3}) [33,34]. Pit proteins are found in all groups of living organisms, including bacteria, archaea, yeast, fungi, plants and animals [35]. The Pit system is constitutively synthesized, and its affinity for

phosphate is 100 times lower than that of the inducible Pst [36]. Cells dependent upon the high affinity Pst system have a Michaelis constant (K_m) of 0.43 ± 0.2 μM Pi (0.013 ± 0.006 g P m^{-3}), which is similar to the value of the phosphate half saturation constant in ASM2 [37]. The above mechanism illustrates that probably under the conditions of this study the Pst system is repressed due to the high orthophosphate concentrations (higher than 31 g P m^{-3} in all bottles) and Pi is thus transported by the constitutive low affinity Pit system. Therefore, the values of the orthophosphate half saturation constant proposed in this study are reasonable. Additionally, since the Pit and Pst systems have different Michaelis constant values, the results obtained in this study should only be considered suitable for anaerobic digesters with high orthophosphate concentrations, which is usual for anaerobic digestion of concentrated sewage sludge, both primary and waste activated. For the situation in which the orthophosphate concentration is lower than 31 g P m^{-3}, further research is needed.

4.3. Simulations

M2 was not able to fit all experimental data as well as M1 did although the values of the non-competitive acetate inhibition constants for fatty acid uptake processes are relatively close to literature data. The reason is that the different uptake rates of LCFA, butyrate (valerate), and propionate at different orthophosphate concentrations were solely the results of the different acetate uptake rates in M2. As shown in Table 3, the $K_{S,po4\_i}$ and $K_{I,po4\_i}$ values of different fatty acid uptake processes were different, indicating that the orthophosphate kinetics on these processes were different. This contributes to the poor model performance of M2, which cannot describe the observation that the orthophosphate effect on the acetate uptake process is different from the effects on the other fatty acid uptake processes.

The result that the AIC value of M3 was higher than that of M1 indicates that model M3 considering both orthophosphate and acetate inhibition did not improve model performance. Because M1 is nested within M3, and M3 is more complex without improved fit, making M3 an unsuitable choice and it is thus more difficult to find a single set of parameters to fit the experimental data. More importantly, orthophosphate but not acetate appears to be the main cause of the different fatty acid uptake rates at different orthophosphate concentrations.

Low TIC values of M1 simulations illustrate that the profiles of variables simulated by the modified ADM1 with Haldane kinetics of orthophosphate inhibition fitted the measured profiles well. Moreover, the pH variations slightly affected the M1 simulations, indicating that the different performances at different orthophosphate concentrations were mainly caused by the different orthophosphate concentrations and not by pH inhibition. Even under non-pH-controlled conditions, the model M1 with the calibrated parameters adequately described the orthophosphate effect on mesophilic anaerobic digestion. The best model fittings were obtained with the Haldane kinetics, an inhibition model where the substrate and the inhibitor are the same substance. On one hand, the availability of phosphorus is an important factor related to bacterial growth. On the other hand, if the orthophosphate concentration is too high, fatty acid uptake processes during mesophilic anaerobic digestion are inhibited according to the experimental results. These results suggest that orthophosphate plays an important role in fatty acid uptake processes, and there is a need to introduce the effect of orthophosphate into the ADM1 model. Since the results are based on a single set of experiments, performed with a single anaerobic inoculum, the model with Haldane kinetics of orthophosphate inhibition together with the proposed parameters should be further validated. Further research with molecular biological techniques is needed to better understand the orthophosphate effect.

5. Conclusions

Batch experiments indicate fatty acid uptake processes are accelerated at intermediate orthophosphate concentrations while a further increase of the orthophosphate concentration slowed these processes down. Based on the experimental evidence, it is proposed to include a new Haldane kinetics of orthophosphate inhibition to the ADM1 model framework. Among three candidate models, this model resulted in the best fits to the experimental results and was validated by additionally considering orthophosphate as a pH buffer. It is worth noting that the proposed model is able to describe the multi-experiment, multi-variable data set so well with a single, common parameter set.

Acknowledgments

This work was supported by the National High Technology Research and Development Program of China (863) (Grant No. 2011AA060902) and the Science and Technology Commission of Shanghai Municipality – China (11230700700). Peter Vanrolleghem holds the Canada Research Chair on Water Quality Modelling.

Appendix A. Supplementary data

Supplementary data associated with this article can be found, in the online version, at http://dx.doi.org/10.1016/j.cej.2014.09.050.

References

[1] A. Oehmen, P.C. Lemos, G. Carvalho, Z.G. Yuan, J. Keller, L.L. Blackall, M.A.M. Reis, Advances in enhanced biological phosphorus removal: from micro to macro scale, Water Res. 41 (2007) 2271–2300.
[2] M. Henze, M.C.M. Van Loosdrecht, G.A. Ekama, D. Brdjanovic, Biological Wastewater Treatment Principles, Modeling and Design, IWA Publishing, London, UK, 2008.
[3] L. Appels, J. Baeyens, J. Degrève, R. Dewil, Principles and potential of the anaerobic digestion of waste-activated sludge, Prog. Energy Combust. Sci. 34 (2008) 755–781.
[4] N. Jardin, H.J. Pöpel, Phosphate release of sludges from enhanced biological P-removal during digestion, Water Sci. Technol. 30 (6) (1994) 281–292.
[5] D.S. Mavinic, F.A. Koch, E.R. Hall, K. Abraham, D. Niedbala, Anaerobic co-digestion of combined sludges from a BNR wastewater treatment plant, Environ. Technol. 19 (1998) 35–44.
[6] W. Rudolfs, G.W. Stahl, Phosphates in sewage and sludge treatment. III. Effects on sludge digestion, Sewage Work J. 19 (1947) 415–422.
[7] L. Van Den Berg, C.P. Lentz, R.J. Athey, E.A. Rooke, Assessment of methanogenic activity in anaerobic digestion: apparatus and method, Biotechnol. Bioeng. 16 (1974) 1459–1469.
[8] Z. Lei, J. Chen, Z. Zhang, N. Sugiura, Methane production from rice straw with acclimated anaerobic sludge: effect of phosphate supplementation, Bioresour. Technol. 101 (2010) 4343–4348.
[9] R. Conrad, M. Klose, P. Claus, Phosphate inhibits acetotrophic methanogenesis on rice roots, Appl. Environ. Microbiol. 66 (2000) 828–831.
[10] J.F. Andrews, Dynamic model of the anaerobic digestion process, J. Sanit. Eng. Div. ASCE 95 (SA1) (1969) 95–116.
[11] J.F. Andrews, S.P. Graef, Dynamic modeling and simulation of the anaerobic digestion process, Adv. Chem. Ser. 105 (1971) 126–162.
[12] D.J. Batstone, J. Keller, I. Angelidaki, S.V. Kalyuzhnyi, S.G. Pavlostathis, A. Rozzi, W.T.M. Sanders, H. Siegrist, V.A. Vavilin, Anaerobic Digestion Model No 1 (ADM1), IWA Publishing, London, UK, 2002.
[13] A. Mottet, I. Ramirez, H. Carrère, S. Déléris, F. Vedrenne, J. Jimenez, J.P. Steyer, New fractionation for a better bioaccessibility description of particulate organic matter in a modified ADM1 model, Chem. Eng. J. 228 (2013) 871–881.
[14] I. Ramirez, E.I.P. Volcke, R. Rajinikanth, J.P. Steyer, Modeling microbial diversity in anaerobic digestion through an extended ADM1 model, Water Res. 43 (2009) 2787–2800.
[15] C.M. Carliell-Marquet, A.D. Wheatley, Measuring metal and phosphorus speciation in P-rich anaerobic digesters, Water Sci. Technol. 45 (10) (2002) 305–312.
[16] Y. Chen, S. Jiang, H. Yuan, Q. Zhou, G. Gu, Hydrolysis and acidification of waste activated sludge at different pHs, Water Res. 41 (2007) 683–689.
[17] APHA, Standard Methods for the Examination of Water and Wastewater, 20th ed., American Public Health Association, Washington, DC, USA, 1998.

[18] R.E. Loewenthal, G.A. Ekama, G.V.R. Marais, Mixed weak acid/base systems part 1 – mixture characterisation, Water S.A. 15 (1989) 3–24.
[19] H. Siegrist, D. Vogt, J.L. Garcia-Heras, W. Gujer, Mathematical model for meso- and thermophilic anaerobic sewage sludge digestion, Environ. Sci. Technol. 36 (2002) 1113–1123.
[20] D. Dochain, P.A. Vanrolleghem, Dynamical Modelling and Estimation in Wastewater Treatment Processes, IWA Publishing, London, UK, 2001.
[21] J. Palatsi, J. Illa, F.X. Prenafeta-Boldú, M. Laureni, B. Fernandez, I. Angelidaki, X. Flotats, Long-chain fatty acids inhibition and adaptation process in anaerobic thermophilic digestion: batch tests, microbial community structure and mathematical modelling, Bioresour. Technol. 101 (2010) 2243–2251.
[22] X. Zhou, A new method with high confidence for validation of computer simulation models for flight systems, Chin. J. Syst. Eng. Electron. 4 (4) (1993) 43–52.
[23] B.K. Ahring, P. Westermann, Product inhibition of butyrate metabolism by acetate and hydrogen in a thermophilic co-culture, Appl. Environ. Microbiol. 54 (1988) 2393–2397.
[24] I. López, L. Borzacconi, Modelling of slaughterhouse solid waste anaerobic digestion: determination of parameters and continuous reactor simulation, Waste Manag. 30 (2010) 1813–1821.
[25] J.B. Van Lier, Thermophilic anaerobic wastewater treatment; Temperature aspects and process stability (Ph.D. thesis), Wageningen Agricultural University, Wageningen, The Netherlands, 1995.
[26] C.Y. Lin, C.H. Lay, Effect of carbonate and phosphate concentrations on hydrogen production using anaerobic sewage sludge microflora, Int. J. Hydrogen Energy 29 (2004) 275–281.
[27] M.G. Lamarche, B.L. Wanner, S. Crépin, J. Harel, The phosphate regulon and bacterial virulence: a regulatory network connecting phosphate homeostasis and pathogenesis, FEMS Microbiol. Rev. 32 (2008) 461–473.
[28] J.F. Martín, Phosphate control of the biosynthesis of antibiotics and other secondary metabolites is mediated by the PhoR–PhoP system: an unfinished story, J. Bacteriol. 186 (2004) 5197–5201.
[29] T.H. Harding, D.S. Ikumi, G.A. Ekama, Incorporating phosphorus into plant wide wastewater treatment plant modelling – anaerobic digestion, in: Proc. 8th IWA Symposium on Systems Analysis and Integrated Assessment (Watermatex2011), San Sebastian, Spain, 2011.
[30] Z. Yuan, S. Pratt, D.J. Batstone, Phosphorus recovery from wastewater through microbial processes, Curr. Opin. Biotechnol. 23 (2012) 878–883.
[31] W. Gujer, M. Henze, T. Mino, T. Matsuo, M.C. Wentzel, G.V.R. Marais, The activated sludge model No. 2: biological phosphorus removal, Water Sci. Technol. 31 (2) (1995) 1–11.
[32] S.G. Pavlostathis, E. Giraldo-Gomez, Kinetics of anaerobic treatment, Water Sci. Technol. 24 (8) (1991) 35–59.
[33] B.P. Surin, H. Rosenberg, G.B. Cox, Phosphate-specific transport system of *Escherichia coli*: nucleotide sequence and gene-polypeptide relationships, J. Bacteriol. 161 (1985) 189–198.
[34] O.A. Vershinina, L.V. Znamenskaya, The Pho regulons of bacteria, Microbiology 71 (2002) 497–511.
[35] F. Santos-Beneit, A. Rodríguez-García, E. Franco-Domínguez, J.F. Martín, Phosphate-dependent regulation of the low- and high-affinity transport systems in the model actinomycete *Streptomyces coelicolor*, Microbiology 154 (2008) 2356–2370.
[36] N.N. Rao, A. Torriani, Molecular aspects of phosphate transport in *Escherichia coli*, Mol. Microbiol. 4 (1990) 1083–1090.
[37] G.R. Willsky, M.H. Malamy, Characterization of two genetically separable inorganic phosphate transport systems in *Escherichia coli*, J. Bacteriol. 144 (1980) 356–365.